DEVELOPING MAGNETIC TWEEZERS FOR CONSTANT LOAD EXPERIMENTS ON MICROTUBULE MOTOR PROTEINS.

BY

SWATI VENKAT

Registration number- 20071045

A Dissertation Submitted to the

INDIAN INSTITUTE OF SCIENCE EDUCATION AND RESEARCH, PUNE,

In Partial Fulfilment of Requirements for the Degree of

Bachelor of Science and Master of Science

In Biological Sciences

August 2011- April 2012

Supervisor : Dr. Roop Mallik.

Host Institution: Tata Institute of Fundamental Research, Mumbai, India.

ACKNOWLEDGEMENTS.

I sincerely thank Dr. Roop Mallik for his guidance throughout this project. I would like to thank Alok Dubey for our many fruitful discussions on the design of the tweezer components. I owe special thanks to Arpan Rai, Ashim Rai and Pradeep Barak for their helpful insights on the design and calibration of the instrument. My sincere gratitude to Rupam Jha, Priyanka Rai, and Kritika Sadh for making my stay in the lab a memorable experience.

I have a sincere debt to the TIFR Central Workshop and Central services for manufacturing all the components required for the successful assembly of the tweezers. Without their diligence, helpful suggestions and patience, reaching this stage of the project would have taken much longer.

My sincere thanks to IISER, Pune for giving me the flexibility to work at the TIFR for my final year dissertation and Dr. Roop Mallik for giving me an opportunity to work in his lab on this project. I thank Dr. Girish Ratnaprakhi, my co-supervisor and Dr. Chaitanya Athale, my Thesis advisory committee member for their support throughout this period.

Last but not the least, I would like to thank my family, my friends at IISER, Pune and my friends at DBS, TIFR for their constant encouragement and support. Without them, none of this work would have been possible.

TABLE OF CONTENTS

LIST OF ABBREVIATIONS

A - Amperes

AFM- Atomic Force Microscope

ATP – Adenosine TriPhosphate

AWG- American Wire Gauge (standardized wire gauge system)

B - Magnetic field

^{0}C - Degree Celsius

CsCl- Cesium Chloride

∇ - Gradient of a scalar function

D.C- Direct Current.

DNA- Deoxyribonucleic Acid

η- viscosity

F- Force, F_m- Magnetic force, F_g – Force due to gravity.

fps- frames per second

γ-Fe_2O_3- Maghemite, magnetic nanocrystals for superparamagnetism

I.D. – Inner Dimensions

m- magnetic moment

M- Molar (moles per litre).

µm- micron

mg- milligrams (10^{-3} gms)

mm- millimetre (10^{-3} metre)

mT- milliTesla (10^{-3} Tesla)

nm- nanometer (10^{-9} metre)

nN- nanonewton (10^{-9}N)

pN- picoNewton (10^{-12}N)

r- radius of a sphere

T- Tesla

t- time (seconds)

v- velocity

V- Volts

LIST OF FIGURES

Abstract

This work reports the construction of magnetic tweezers that can apply a spatially uniform magnetic force on superparamagnetic beads viewed in an optical microscope. The apparatus, constructed and assembled on the current microscope setup is composed of 2 electromagnets and can exert a constant force along an axis perpendicular to the generated field. The instrument was calibrated by measuring the velocity of single 2.8μm dynal magnetic beads near the surface since magnetic beads eventually sink to the surface due to their high density (1.6gm/cc). The maximum magnetic force on the beads, determined using Stoke's law was found to be 7.29pN at 1.6A current with a spatial variation of 4%. However, since beads near the surface experience higher drag force than the value determined using Stoke's law, the magnetic force on these beads is higher than estimated. Further work aims to calibrate neutrally buoyant beads suspended in a 3.9M Cesium Chloride solution of equal density (1.6gm/cc). The calibrated instrument will then be used to investigate the nature of single and multiple dynein-driven magnetic phagosome motion in response to constant load.

Chapter 1: INTRODUCTION

Forces and motion are fundamental to all biological systems and single molecule manipulation has become vital to probe the physical underpinnings of such biological motion. In recent years, various single molecule techniques such as AFM, optical tweezers and magnetic tweezers have been developed for a wide range of biophysical research (K.C. Neuman et al., 2007, Veigel and Schmidt, 2011). Although ensemble biochemical analysis is integral to obtaining qualitative as well as quantitative descriptions of the system, it can rarely outline details pertaining to molecular phenomena (R.Conroy,). Single molecule force spectroscopy has therefore emerged as an important and powerful tool to explore molecular dynamics, structure variation and interactions so as to provide a clearer understanding of the bigger physiological picture (Neuman and Nagy, 2008).

Magnetic Tweezers

A magnetic tweezer is a device capable of exerting forces of precise magnitude and direction on magnetic particles (Vilfan et al., 2009). Given their relatively low cost of construction and ease of operation, magnetic tweezers have, in recent times, emerged as a versatile device to probe the physical properties of biological systems such as viscosity (Bausch et al., 1999) or forces exerted by motors such as DNA topoisomerases (Strick et al. 2000) and kinesin (Fallesen et al., 2010) The idea of using magnetic fields to probe biological systems dates back to Crick and Hughes' work in 1950 which involved manipulating iron rust in chick fibroblasts to study the viscoelastic properties of cell cytoplasm (Crick and Hughes, 1950). Magnetic tweezers selectively act on magnetic particles and thus involve introducing magnetic particles into the system under study.

The basic design generally consists of a pair of electromagnets or permanent magnets placed above the sample holder of a microscope and can be designed to exert forces typically in the range of pN to nN so as to rotate or translate micron-sized magnetic beads (Neumann and Nagy, 2008). They are highly selective and unlike AFM or optical traps (S.P. Gross, 2003), where the force varies with displacement, magnetic tweezers can be designed to exert constant forces over

relatively large areas (Fallesen et al., 2010), making it a suitable device to investigate molecular dynamics under constant force.

Motivation

One of the interests of our lab is to study the behaviour of microtubule motor proteins such as kinesin and dynein, using biophysical assays. There is a lot to be learnt about the mechanics and kinetics of these motors, especially dynein (Gee. M and Vallee R., 1998). It has been shown that dynein can work as a gear in response to load- an external backward force on a bead attached to a motor which traverses on the microtubule. This was exerted using an optical trap. (Mallik et al. 2004).

However, the force exerted by an optical trap varies as a function of distance of the trapped particle from its mean position. Hence, any change in the step-size of dynein would be simultaneously accompanied by a change in the load, and therefore the behaviour of dynein as a gear is not strictly in response to a constant load. A magnetic tweezer however, can exert a precise, constant force over areas greater than typical cellular dimensions (Hosu et al., 2003). This allows us to study the behaviour of motor proteins under constant load independent of displacement. Another advantage it would have over an optical tweezer is that many magnetic beads will be subject to the same force over a given area allowing us to visualize their behaviour simultaneously.

The goal of this project is to develop magnetic tweezers which can be used to study the behaviour of dynein under a constant load. The force will be exerted on dynein via its magnetic load i.e. magnetic phagosomes. Motile magnetic phagosomes can be manipulated by magnetic tweezers to gain insights into motor behaviour under constant load. It is known that dyneins commonly work in groups to execute cellular functions () as opposed to working individually. Future studies also aim to investigate the role of dynein’s gear mechanism in working efficiently as a team to carry out their functions.

Magnetic tweezers- Working principles and design considerations

Force on a magnetic bead

The force acting on a paramagnetic bead with magnetic moment **m** due to a spatially varying field **B** is

$$\vec{\mathbf{F}}_{\mathbf{m}} = \nabla(\vec{\mathbf{m}}.\vec{\mathbf{B}}) = \nabla(\mathrm{mB}) \qquad (1)$$

(second equality occurs because the induced moment in the bead is parallel to the magnetic field B.). This equation quantifies the force generated by the magnetic tweezers on magnetic beads of our interest. Typically, paramagnetic beads, depending on size, contain 10^6 γ-Fe_2O_3 nanocrystals with an average diameter of 8nm dispersed in a polystyrene matrix and coated with a polymer coating (Fonum et al. 2005). The distance between iron oxide particles and their size is precisely controlled to make them superparamagnetic (Bean and Livingston, 1958)

Dynein motors have been shown to stall at ~ 1.1pN of force in-vitro (Mallik et al. 2004, Manoranjan et al., 2005) and multiple dynein motors acting in groups of 4-5 are capable of generating forces upto 4.4-5pN in-vitro (Soppina et al. 2009). The device should therefore be designed to exert a similar range of forces on magnetic beads so as to effectively study the workings of single and multiple dyneins under load.

Magnetic beads

The magnitude of force exerted by a tweezer would depend on the magnetic properties of the bead, and therefore its magnetic moment **m**. An important consideration is the magnetic moment $\mathbf{m_s}$ (when the magnetization of the bead is saturated) of M270 Dynal beads (Invitrogen), which we will be using for force calibration of the tweezers. (Fig. 1.1) shows the magnetization curve of 2.8μm Dynal beads (Fonnum et al. 2005). The magnetic moment of these beads, $m_s = 1.9 \times 10^{-13}$ Am^2 (Fallesen et al., 2010) ensures that fields in the range of 200mT-500mT can exert relevant forces in the order of pN on these beads.

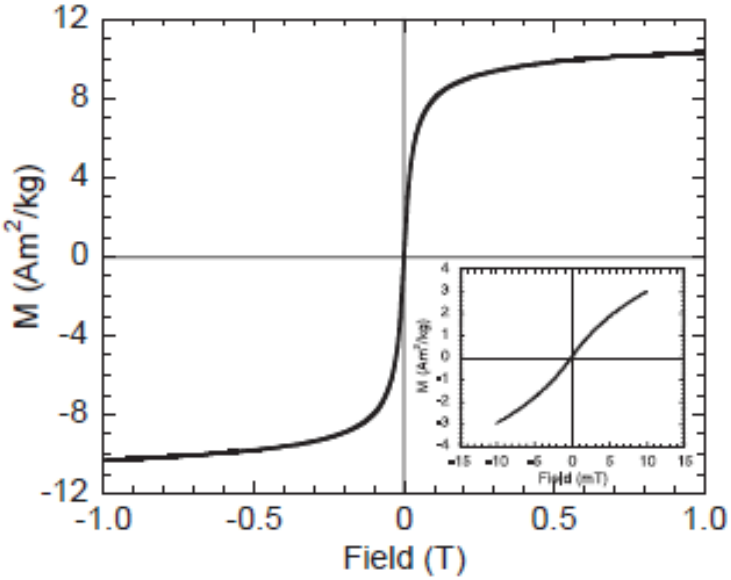

Fig.1.1- Magnetization vs Magnetic field for 2.8μm Dynal beads. Saturation of the bead occurs at ~ 0.1T (Fonnum et al. 2005).

Before saturation (B<~100mT), magnetic force F_m α $(\nabla B)^2$, since m increases approximately linearly with B. However, once the bead is saturated it can no longer be magnetized further, i.e. m=m_s. The magnetic force on the bead now will vary as a function of the gradient of the field (since m becomes independent of B) i.e. $\mathbf{F_m}$= m_s (∇B). This is an important consideration for the design of pole piece geometry (described in the following section) that should be able to generate a field profile that can exert constant forces on the superparamagnetic beads i.e. F_m= $\nabla(\mathbf{m}B)$= constant.

Constant force profile

A constant force implies a uniform gradient of field according to (1). Therefore the surface of permanent magnets or the core of the electromagnets from where the major density of field lines emerge (will be referred to as pole pieces in the following sections) must be machined to a specific geometry that can establish the required field profile. Various pole piece designs have been implemented to attain high or constant forces, the gradient being perpendicular to the direction of the magnetic field. Faraday pole piece (A Rais and A A Yousif (1999), M. Garber et al. 1960, Soule et al. 1964) is a commonly implemented pole piece design to attain constant forces in the pN range. However a recent study by Fallesen at al. 2010,

demonstrated a novel pole piece design which can generate constant forces upto 12pN at 1500 Ampere turns (current x no. of windings in the electromagnet coil) over an area of 4mm x 0.5mm, which we decided to adopt for our tweezers (described in Chapter 2).

Design Considerations

The construction of magnetic tweezers on the existing microscope set-up requires the following design considerations (Hosu et al., 2003):-

1. Constant force or field gradient (implying uniform magnetic field variation) over ~100μm x 100μm area.
2. Precise direction of force along the wedge-shaped gap of the pole piece.
3. The field should be strong enough to magnetize the superparamagnetic beads to saturation. This maintains constant magnetic moment '**m**' for the bead, which assures constant force with the adopted pole piece design.
4. The design should fit on the existing microscope without disrupting the functionality of the existing instrument setup.
5. Sufficiently rapid and accurate adjustment of force should be possible during experiments.
6. Magnitude of forces attained should preferably reach ~7-8pN for usage in subsequent motor protein experiments.

This report details my work on the design, construction, assembly and calibration of the instrument on the existing microscope set-up.

Chapter 2: MATERIALS AND METHODS.

The instrumentation primarily involved 4 steps-

1. Designing the magnetic tweezer components and a suitable sample holder to accommodate the tweezer set-up.
2. Manufacture of the components (carried out at the TIFR Central Workshop and Services.).
3. Assembly of the components onto the existing Nikon microscope.
4. Calibration of the instrument using M270 Dynal beads.

Principles and design considerations.

We decided to use electromagnets as opposed to permanent magnets since electromagnets yield the advantage of having a precise control of magnetic field with current. Additionally, handling and machining strong permanent magnets (neodymium, boron or iron) into a specific geometry so as to generate the required field profile is difficult.

Electromagnet Coil

The coil of each electromagnet comprised of 750 turns (uniform winding) of 24 AWG (0.511mm diameter) magnet wire. The strength of the magnetic field of a solenoid depends upon the number of Ampere turns i.e. Current x Number of turns of the coil. Since we wanted to limit the current to a maximum value of 2A, we decided to increase the number of turns (750 turns) so as to attain the required field strength. The choice of wire was based on its capacity to sustain high current (> 10A) for extended periods, optimize heating effects and limit the number of layers during winding to a feasible value. This winding was carried out over a length of 21mm amounting to 16 layers of wire.

Bobbin design

In order to hold these layers in place, a bobbin was designed as shown in Fig. 2.1. Design considerations included that the structure be light, withstand high

temperatures (therefore bobbin was made of Bakelite), accommodate approximately 1.2cm height of wire on each side and be conveniently suspended so that the pole piece protruding from the core can be finely adjusted to reach the field of view of the objective (Fig. 2.2).

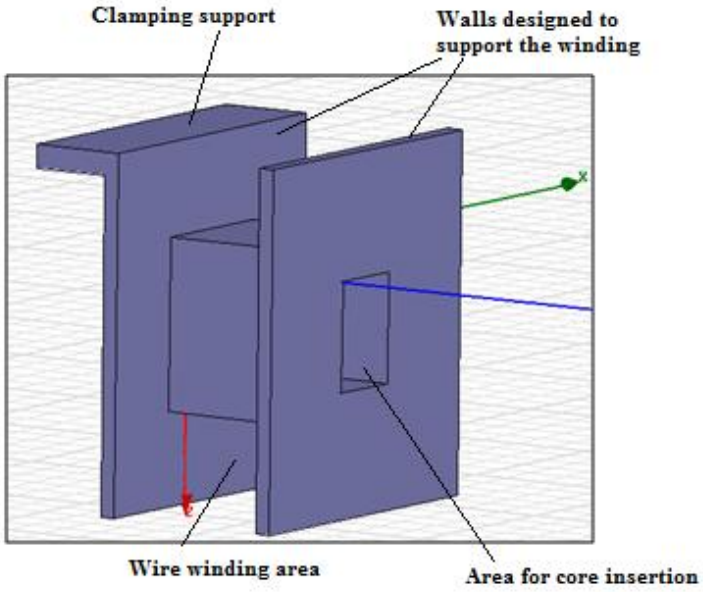

Fig.2.1- Bobbin design - The core was inserted into the hole at the center. The coil was wound between the 2 walls which supported the 16 layers of winding. The whole electromagnet (weighing ~ 200gms) was suspended from an aluminium block via the clamping support.

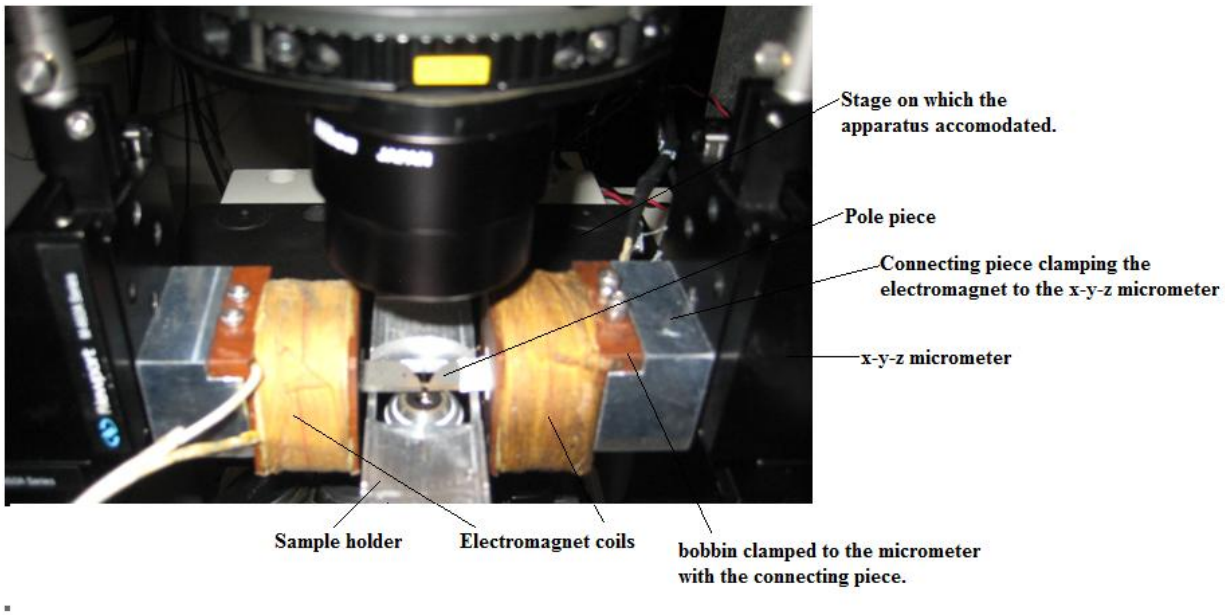

Fig. 2.2- The tweezer set-up on the microscope.

Electromagnet core

The core material was 3% grain-oriented silicon-iron steel (Kryfs Power components Ltd.), 0.3mm thick sheets (AK Steel product data bulletin- Oriented M-5 CARLITE). Choice of this material was based on its high permeability, high saturation value (1.8T) as well as ease of availability. Each core comprised of 30 sheets of dimensions 10mm X 25mm, stacked over one another and glued to each other with high-temperature resistant araldite (AV-138, HV-998, Variety Plywood, India). The centre of the core comprised of longer sheets of a specific geometry (Fallesen et al., 2010). The major design consideration of the core was that the pole pieces protruding 1cm out of the bobbin (Fig. 2.3) should form the middle of the core of stacked sheets. The geometry of the pole piece is integral to the field profile obtained.

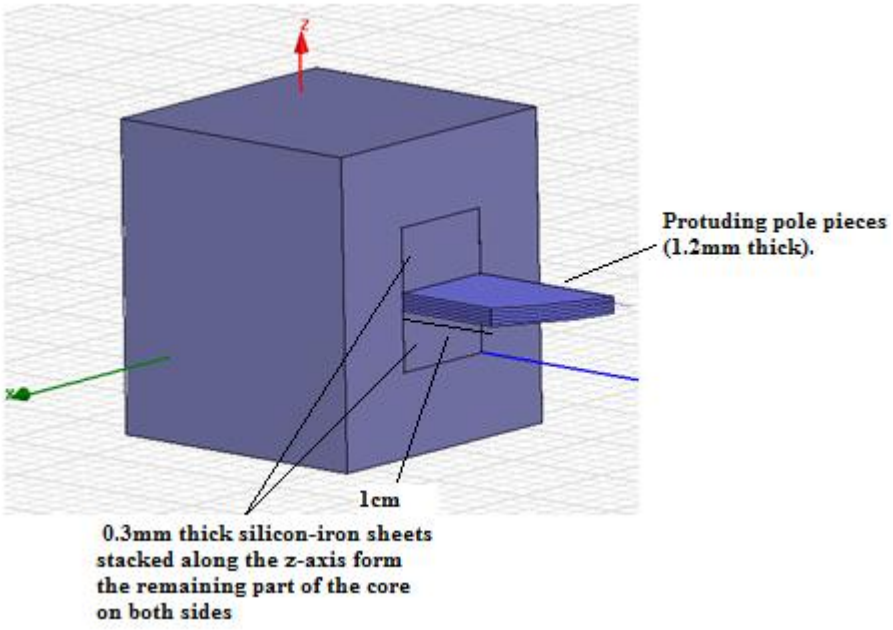

Fig.2.3- Protuding pole pieces form the centre of the electromagnet and concentrate the field lines at their ends within a small region.The coil is represented simplistically as a rectangular box.

Pole piece design

The pole piece geometry was chosen by studying literature on different pole piece designs implemented by groups developing magnetic tweezers for specific applications. (Gosse and Croquette, 2002, Hosu et al., 2003, Fallesen et al., 2010).

A primary requirement for our experiments is a constant field gradient, i.e. a constant force in order of pN generated over areas of typical cellular dimensions. Recently Fallesan et al. implemented a novel design, to generate the required constant forces over an area of 4mm x 0.5mm, that can magnetize a large number of beads in a given field of view at once and therefore is more convenient to work with under the microscope. Their design emphasis was to obtain a large and constant value of the magnetic field gradient (∇B) where in B_x> 100mT within the gap between the pole pieces. The shape of the pole pieces they found best was an arc of radius 20mm, with its centre 4mm outside the edge of the pole piece (Fig. 2.4). We decided to adopt this design for our tweezers.

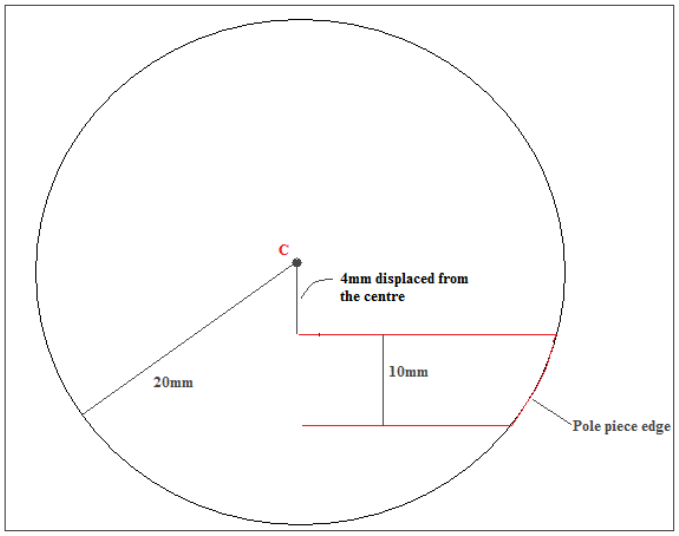

Fig 2.4- Geometry of the pole piece adopted for the tweezers.

Each pole piece was made up of 5 silicon-steel pieces (0.3mm thick), machined at the central workshop. They were stacked over each other and glued, comprising the middle section of each core. The thickness of the pole piece 1.5mm, was primarily dictated by the working distance of the objective. The advantage of having a considerable z-dimension is that edge effects in the z-axis are minimized by placing the sample at the centre of the pole piece thickness.

Power supply

The two electromagnets were powered separately using independent channels of an 18V-5A dual channel programmable D.C power supply (Aplab-PPD-1805). The supply was operated in constant current mode up to an accuracy of 0.01A

Sample Holder design

The existing Nikon sample stage was replaced by a non-magnetic aluminium design which can accommodate capillaries, petridishes and slides in the same holder. This design was essential because the previous set-up could not accommodate a set of electromagnets within a range of 1mm from each other and a capillary tube within this gap in the same plane as the pole pieces.

The width of the sample holder was limited by the proximity of the electromagnets, while the thickness was contingent on the dimensions and working distance of different objectives being used, and to simultaneously maintain the freedom of the objectives to rotate (freedom of rotation allows the user to alternate between different objectives conveniently.). The length of the holder was optimum to reach the field of view of the objective and ensured no visible (under a 100X objective) vibrations in the z-plane (given that it was attached in suspension from the fixed micrometers). The groove for the capillaries was designed to accommodate 50mm x 0.3mm x 0.3mm I.D. capillaries (Fig. 2.5).

Apart from the sample holder, 2 pieces were designed to suspend the sample holder from the micrometer stage at the appropriate height and area (Fig. 2.7)

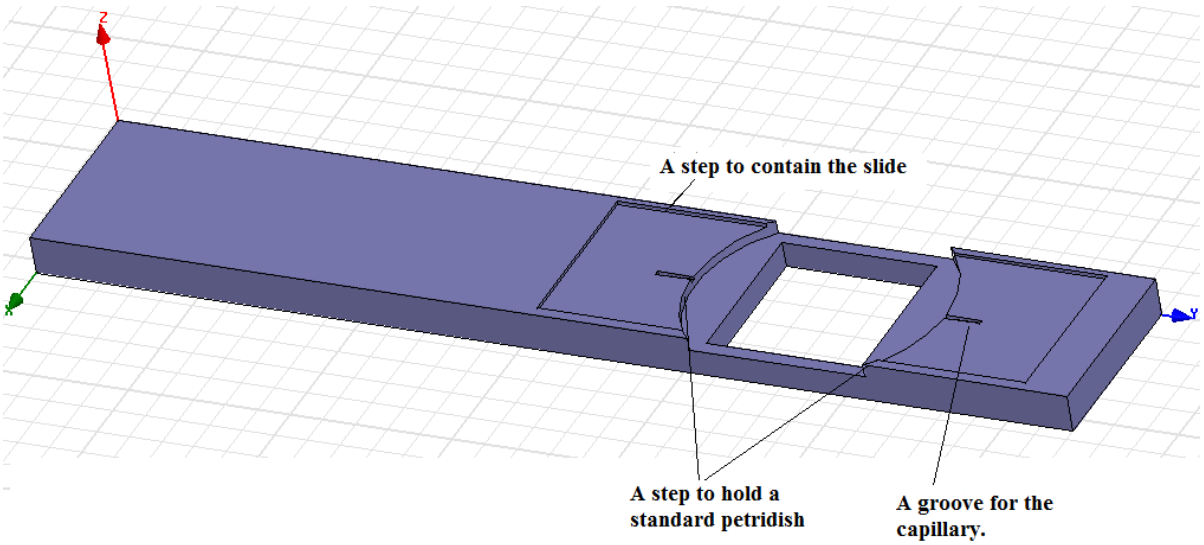

Fig.2.5 shows the final sample holder design.

The pole pieces are generally separated by a distance of 1mm from each other to generate forces of pN range. Therefore, we decided to carry out experiments in capillary tubes (Vitrocom Inc., NJ) of 50mm X 0.3mm X 0.3mm I.D and having a wall thickness identical to that of coverslips. This would be placed at the centre of the wedge-shaped gap, the longer axis being aligned along the x-axis of the gap (Fig. 2.6)

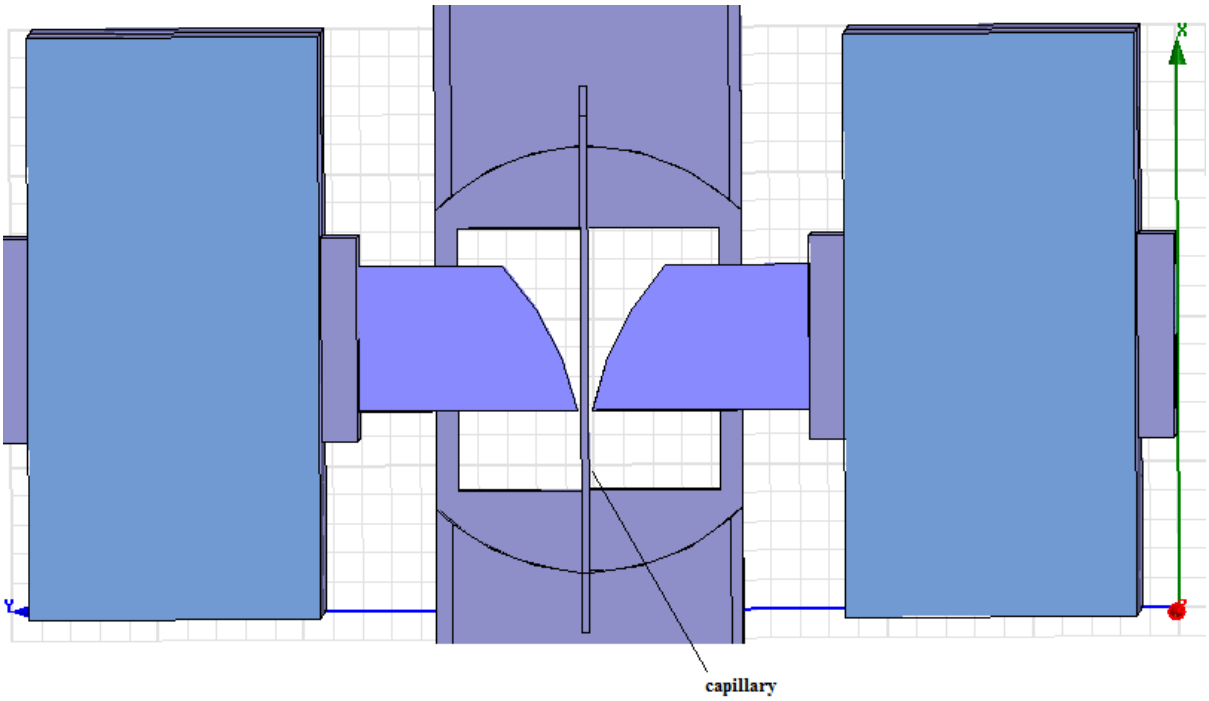

Fig. 2.6- Placement of the pole pieces with respect to the sample holder (not drawn to scale). Experiments are carried out in the capillary tube placed along the length of the gap.

All designs of the sample holder and the electromagnet were drawn in Ansoft Maxwell 13.0. The bobbin, silicon-steel core components, pole pieces, the sample holder and the connecting pieces were manufactured at the TIFR central workshop.

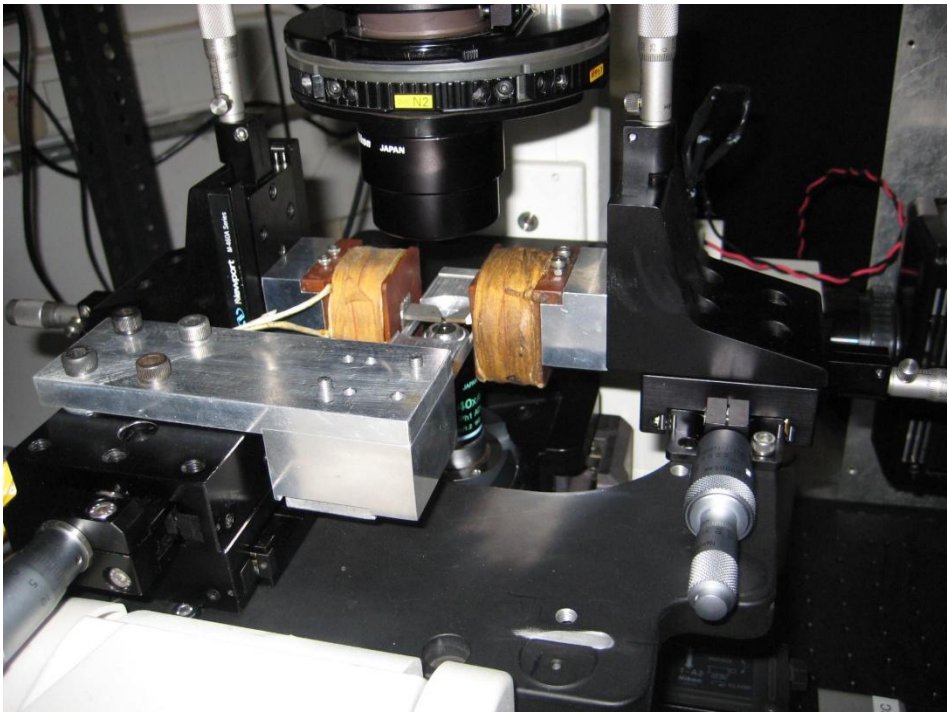

Fig.2.7- The tweezer component assembly on the stage. The setup is symmetric about the stage centre.

Assembly of Magnetic tweezers components

The components of the prototype had to be assembled on the existing microscope. This involved the following :-

1. Fine adjustment of the electromagnets in the x,y,z axes so as to align the ends of the pole pieces suitably in the field of view of the objectives. Integral to this is the design of connecting pieces and the bobbin of the electromagnet so as to allow attachment of the electromagnets to appropriate micrometer stages that control such movement.
2. Fine adjustment of the designed sample holder so as to place it in the field of view of the objective in x, y, z directions. This involved designing non-magnetic aluminium supports that suspend the sample holder from the micrometer stage at the appropriate height and distance. The design must also ensure the stability of the suspended sample holder.
3. A stage which allows the components with above stated requirements to be accommodated on the existing microscope. Freedom of rotation of objectives of the microscope must prevail after assembly of components on the stage.

Two x-y-z micrometers (Newport Corp., CA) were clamped symmetrically on each side of the stage as seen in Fig. 2.7. The micrometers can support a maximum movement of 1cm along each axis. A connecting piece made of non-magnetic aluminium was clamped to each micrometer, to which the bobbin was clamped in suspension (Fig. 2.7). The stage on which the components were assembled was a component of original Nikon base stage. It was well suited for the present purpose of assembling these components as well as permitting the required rotation of the objectives.

The sample holder was suspended at the centre using an x-y micrometer (Jain LABTECH, India), having a degree of freedom of 2 cm along each axis. The suspension was achieved by designing 2 aluminium blocks (Fig. 2.7), manufactured at the TIFR workshop with precision to ensure that the perpendicular and parallel components can be clamped with accuracy.

A caveat of this assembly is that the pole pieces cannot be move much farther apart (maximum separation ~ 1.2cm) from each other along the y-axis, making it difficult to view samples on glass slides/petridish (in experiments not involving the tweezers) without disturbing the relative position of the pole pieces with respect to each other in all 3 axes. A way to circumvent this can be to make use of micrometers with extended ball bearings (clamped much farther from each other than at present) which would allow greater separation of the tweezers in the y-axis without disturbing their relative position along x and z axes, simultaneously allowing visualization of slides/petridish samples.

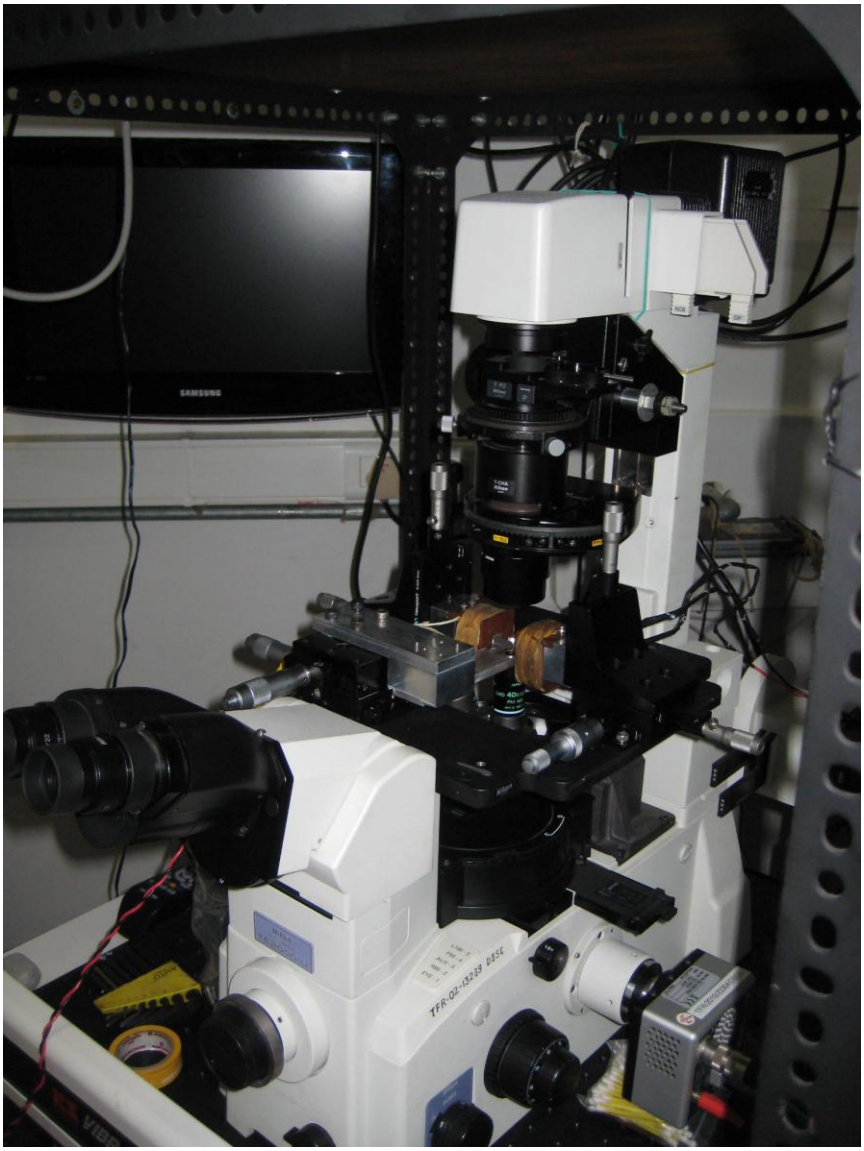

Fig. 2.8- Position of the tweezer with respect to the Nikon microscope.

Performance of the Magnet

Fallesen et al. found the area from x= -5mm ± 1.5mm as a suitable region where the gradient of the field remains nearly constant (Fig. 2.9) The above assembled system was simulated in Ansoft Maxwell 13.0 to confirm the magnitude as well as region of constant gradient for varying values of current, the designed electromagnet configuration, and the given pole piece geometry. The simulation at 1200 Ampere turns i.e 1.6A indicated a gradient of 48.45mT (Fig. 2.10), which would result in a force which can be theoretically computed from Eqn. (1) as

$$\mathbf{F} = m.(\nabla B) = 1.9 \times 10^{-13} \times 48.45 Tm^{-1} = 9.2 \text{ pN}.$$

The performance of the magnet was not assessed empirically at different x-values along the centre of the wedge-shaped gap since the hall probe was too thick to fit in between a 1mm gap.

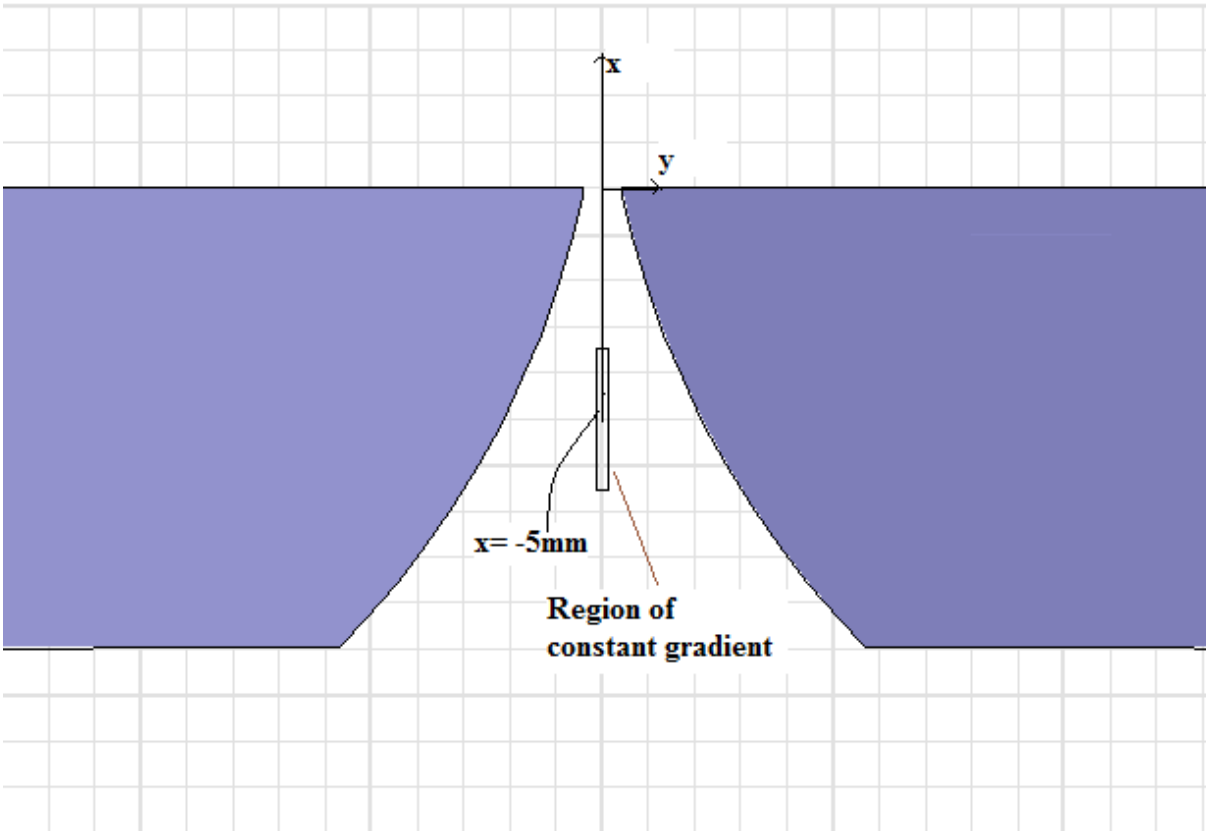

Fig. 2.9- Area of constant gradient at x= 5mm ± 1.5mm, measuring 500µm (-250µm to +250µm) along the y-axis. The centre of this region is along the line at the centre of the symmetric pole pieces as shown.

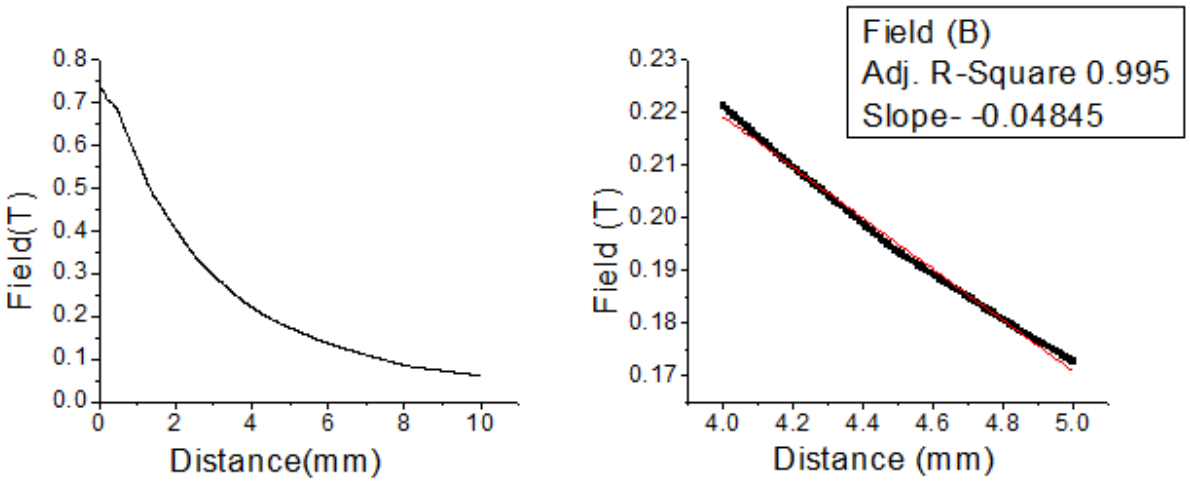

Fig. 2.10- Magnetic field B as a function of distance along the x-axis at 1200 Ampere turns- simulated in Ansoft Maxwell 13.0. The figure to the right represents the area from x=-4mm to x=-5mm, where the field gradient is relatively constant and is the region where subsequent calibrations were conducted.

The performance of the magnet was therefore assessed in the area x= -5mm +1.5mm, (the pole pieces ~ 950µm apart) by measuring the magnitude and direction of force on Dynal M270 (Invitrogen) superparamagnetic beads

Bead tracking and force estimation

Velocity of single Dynal beads in 1.2 M sucrose solution (~ 41% weight sucrose) at 25^0C was measured as a function of current to determine the magnetic force F_m on each bead. The velocity was measured at 0-1.6A current at intervals of 0.4A. The capillary tubes were coated with 5 mg/ml casein half an hour prior to flowing in the 1.2M sucrose+ beads solution. This ensured efficient blocking of the capillary walls that prevented the beads from sticking to the surface. The ends of the capillary were sealed with vaseline to prevent it from drying. The drag force F on the beads can be determined using the Stokes relation :-

$$F= 6\pi\eta rv \qquad (2)$$

Where η is the viscosity of the solution~ 0.005164 $kgm^{-1}s^{-1}$ at 25^0C, r- radius of the bead= 1.4µm, v is the velocity of the bead. If the beads move with a constant velocity over the region of our interest, it implies that net force on the beads is 0. Thus the magnetic force (F_m) can be equated to the drag force (F_d) on the bead, which is determined using equation (1).

The bead was video-tracked over an area of 120µm x 120µm, i.e. x= -5mm +120µm; y~ +30µm to +150µm (Refer Fig.2.9.). This area was within a capillary of I.D 300µm x 300µm, which was placed at the centre (with reference to the y-axis) by viewing its relative positions with respect to the pole pieces under a 10X objective. The z-position of the capillary was adjusted to be placed at the centre of the pole piece thickness. Video tracking of the beads was done with a Nikon microscope, 40X Ph1 objective, Cohu camera (Cohu Inc., CA, 30fps) and recorded using the AVI

tracking program, coded in LabVIEW 8.6 by Roop. 5 beads were tracked for each current value to calibrate the trap.

Direction of bead motion

The x-y trajectory of the beads was analyzed to determine the direction of magnetic force. A low slope in the x-y graph would indicate relatively straight motion of the beads along the positive x-axis (Refer Fig. 2.9) which would match the expected direction of F_m ((Refer (1)).

Bead motion in the z- plane

While measuring the magnetic force on the beads, it was noticed that the magnetic beads settle down eventually because they were heavy (density of 1.2M sucrose solution is 1.17439 gm/ml which is much lower as compared to the density of beads which is 1.6gm/ml) and possibly because of some issues regarding uniformity of the field along the z-axis. We could not empirically measure the field along the z-axis since the hall probe was too large to accurately measure the variation of the field over a 1.5mm distance. Simulating the system however showed a field profile along the z-axis at 1200 Ampere turns (Fig. 2.11) i.e. 1.6A current. The field increases till ~0.5mm and then decreases, implying that at around this point the force along z (slope of the curve) must reduce to 0. However, since we have used 1.2M sucrose solution, the bead will tend to sink due to gravity, and thus in order to understand the role of the field along the z-axis, the bead force must be calibrated in a solution of equal density to prevent sinking of beads due to gravity.

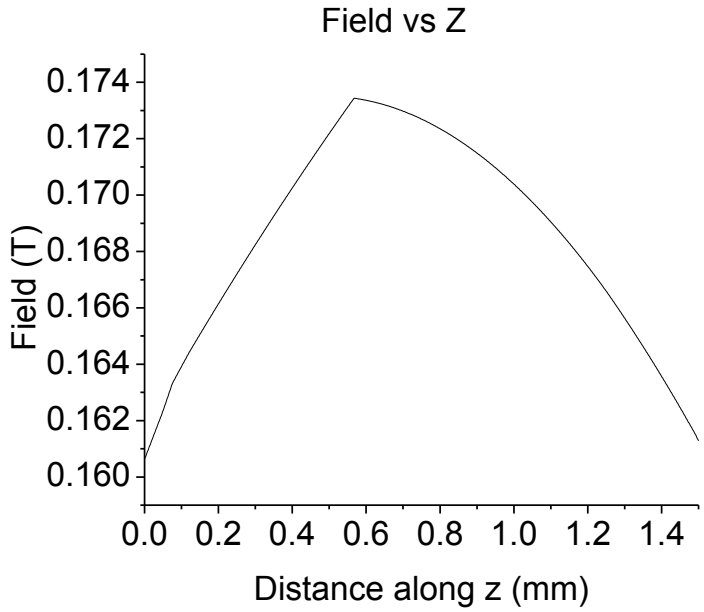

Fig. 2.11 – Field profile along the z-axis (i.e. into the plane of paper in Fig. 2.9) at x= -5mm, 1200 Ampere turns, simulated in Ansoft Maxwell 13.0.

The initial force calibration was therefore performed by recording the velocity of the beads moving near the capillary surface. This however may be an underestimation of the actual magnetic force exerted since friction and higher viscosity near the capillary walls slow down the beads greatly. Experiments to obtain accurate estimates are an immediate priority and will be carried out by immersing beads in an equally dense 3.9M Caesium Chloride (CsCl) solution (density= 1.6gm/ml) to keep the beads neutrally buoyant.

Chapter 3: RESULTS AND DISCUSSIONS

(A) Results

Direction of magnetic force – It is important to ascertain the direction of magnetic force on the beads. In subsequent biophysical assays, microtubules will be present horizontally on the capillary surface along which the motors will generate force to move. Experiments on motor proteins will focus on microtubules oriented in a specific direction, preferably parallel to the x-axis in the wedge-shaped gap. A magnetic force not strictly parallel to the x-axis implies that the estimated force (computed by recording bead velocity) has components along other axes, which would change our estimate of the magnetic force along the direction of motor movement. Therefore, it is important to calibrate the magnitude of force that the instrument can apply along this direction (x-axis). Any component of magnetic force in a direction other than +x-axis will be evident through deviations in trajectory of the beads from the x-axis.

The x-y trajectory of single beads as a function of current- A representative graph of the variation of bead motion in y as it moves along the x-axis at 1.0A current (Fig. 3.1). 5 beads were tracked for every current value over ~ 14400μm^2 area. The maximum y deviation for every bead remained well within 5 % of the x distance travelled i.e. tan(y/x) < 0.05 (maximum deviation obtained was 4.3% for one of the beads at 1.6A current). 22 out of the 25 total beads tracked showed a deviation less than 2.5%.

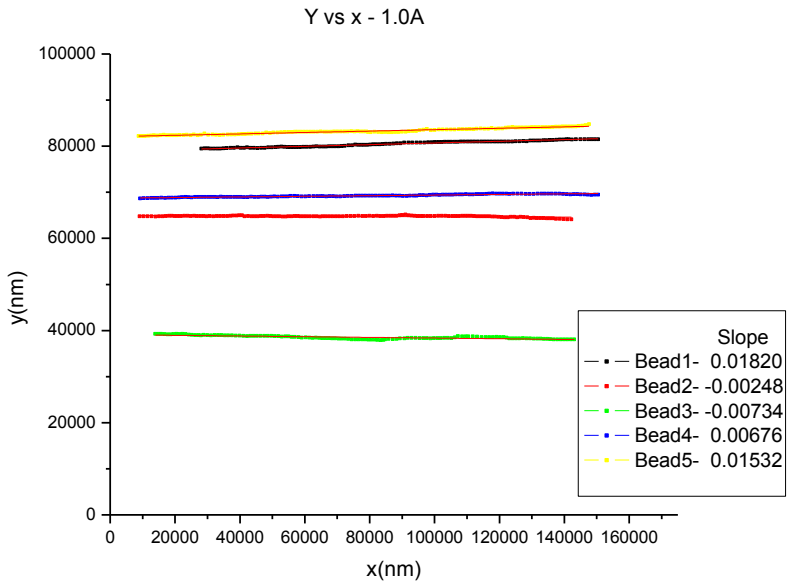

Fig. 3.1 represents the deviation of the bead in the y direction as it moves along the x-axis.

As mentioned, the slopes representing this deviation are well within a 5% deviation i.e. there is not more than a 3^0 deviation from the x-axis. This would imply that a net force of 6pN measured on the beads would be equivalent to a force of 6 * cos(3)= 5.991pN along the x-axis, leading to a maximum of 0.15% error in force measurements. A y-component of 6 * sin(3)= 0.314pN will also experienced by the beads which may not pose a significant problem if the motility experiments are performed on microtubules parallel to the x-axis.

Magnitude of magnetic force on beads at the surface- The following Fig. 3.2 is a representative graph of the velocity of 5 beads measured at the surface at 1.0A current.

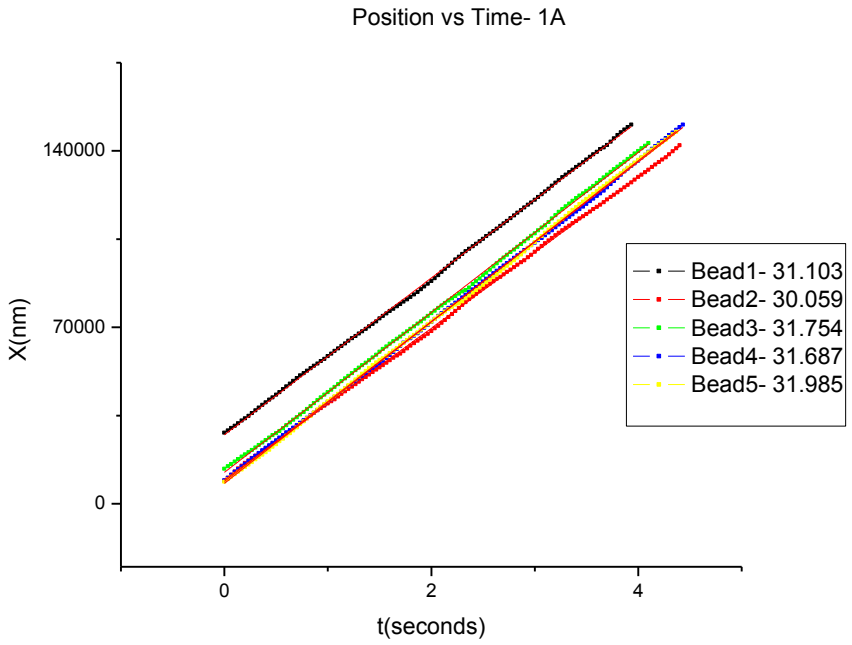

Fig. 3.2- Position vs time graph, the slope of which gives the velocity of the beads represented in the legend. The average velocity is 31.31µm/s.

The average velocity of single beads at 1.0A current (when measured at the surface) is 31.31µm/s ± 0.775µm/s. A plot of the bead velocity as a function of current (Fig. 3.3) gave a velocity of 53.64µm/s ± 2.14µm/s at maximum tested current value of 1.6A. The maximum standard deviation in velocity across beads was 6% at 0.4A current i.e. 8.48µm/s ± 0.4992µm/s. Bead velocity at the surface varies almost linearly as a function of current.

Since the velocity is fairly constant over 120µm, the net force on the bead is 0 i.e. the magnetic force and the opposing drag force are equal. Consequently, the magnetic force on a single bead moving at the surface as a function of current was calculated using the Stokes law. A force of 7.29pN ± 0.29pN was obtained at the maximum tested current value of 1.6A (Fig. 3.4), which is lower than the simulated value of 9.2pN. Given that velocity linearly varies with force ($6\pi\eta rv$), the estimated force shows a fairly linear increase with increase in current upto 1.6A.

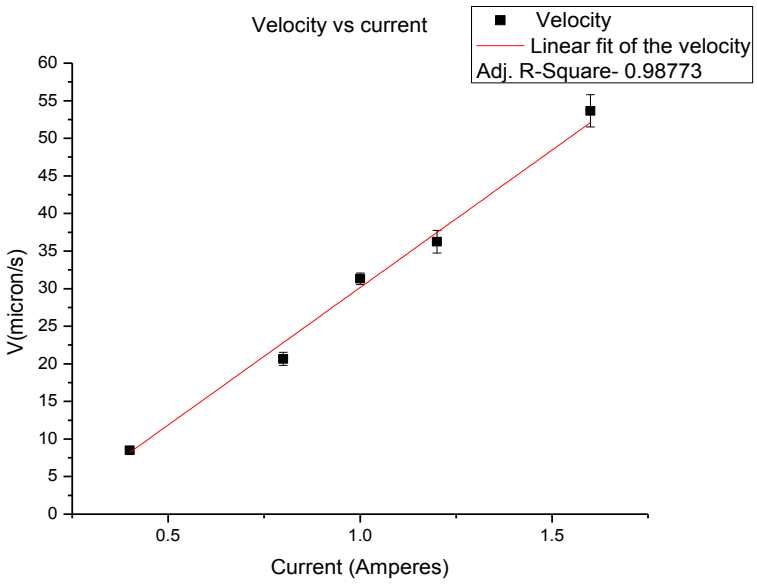

Fig. 3.3- Velocity as a function of current, the maximum velocity is 53.64µm/s ± 2.14µm/s at 1.6A current.

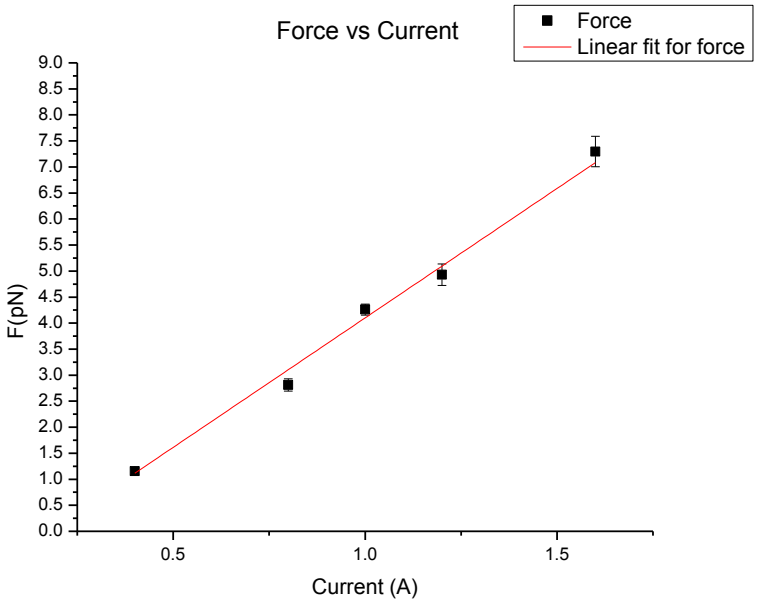

Fig. 3.4- Force as a function of current. Maximum force is 7.29pN ± 0.29pN at 1.6A current.

The variation of velocity within a single bead over ~ 120µm was determined. Velocity by considering pairs of frames separated by 0.3s was calculated over the 120µm distance. The maximum standard deviation in within-bead velocity over 25 beads was 4.23µm/s, the average deviation being 1.64µm/s. The 4.23µm/s variation of velocity within a bead can be attributed to due to frictional contact of the bead with

casein on the capillary surface, which might have caused the beads to slow down or accelerate erratically. Calibration experiments with neutrally buoyant beads in 3.9M CsCl solution would help us understand the causes of this variation better.

(B) DISCUSSIONS

In summary :-

1. The force on the beads is found to be constant, with a maximum variation of 5% over a region of ~14400μm^2, in a direction along the x-axis.
2. The maximum force on a single bead moving at the surface was found to be 7.29pN± 0.29pN at 1.6A current.

Force Estimation.

2.8μm Dynal beads are heavy and eventually settle down to the capillary surface. The bead in solution primarily experiences 3 forces along the z-axis as it settles 1. Force due to Gravity (F_g) 2. Viscous drag force due to the sucrose solution 3. Buoyant force due to the sucrose solution (F_b). We can estimate the time taken for the beads to settle on to the lower wall of the capillary from a height of 100μm above the surface:-

$$F_g - F_b = mg - v\rho g = [((4/3)\pi r^3 \times 9.8 \times (d - \rho)$$

$$= 1.14 \times 10^{-17}\ m^3 \times (1600 - 1174)\ kgm^{-3} \times 9.8\ ms^{-2}$$

$$= 4.759 \times 10^{-14}\ N$$

Here, d is the density of the bead, ρ is the density of the 40% sucrose solution. Assuming no acceleration of the bead or thermal forces, this force can be equated to the viscous drag force $6\pi\eta rv$, which yields a velocity of 0.349μm/s in a 1.2M sucrose solution. This would cause the beads to settle down due to their weight in ~ 4.7mins when 100μm above the surface. The calibration was carried out when most beads settled down.

The estimated force may be an underestimation of the force exerted on the beads by the tweezer, since the beads tracked are ones rolling on the surface. It was found that beads which were deeper inside the solution, moved much faster. However,

such beads became defocused (in the z-plane) almost immediately after being subject to a force and moved slowly once they reached the surface. It was therefore difficult to track them.The reason for their movement along the z-axis might be due to a force along the z-axis as mentioned before, and also because the beads are heavy and would eventually move along the lower surface due to their weight. In any case, the velocity of the beads at the surface is not a true indication of the actual force exerted and needs to be corrected for.

Faxen correction

Many theoretical corrections have been introduced to the drag force experienced by a sphere near the surface or a wall. This discrepancy from the drag force given by the Stoke's law is attributed to 'wall effects' (Happel J. and Brenner H., Kluwer, Drodchet 1991) - hydrodynamic interactions between the flat wall and the colloidal sphere. The drag force on a sphere in an unbounded case therefore, is much different from the case when the spherical bead is rolling on a flat surface (Chungil Ha et al., 2009). In 1924, Faxen derived a single sphere's hydrodynamics near a rigid planar surface. The magnitude of drag force F_d parallel to the flat wall in this case is given by the Eqn (3) below:-

$$\frac{6\pi\eta r v}{1-\left(\frac{9}{16}\right)\left(\frac{r}{h}\right)+\frac{1}{8}\left(\frac{r}{h}\right)^3-\frac{45}{256}\left(\frac{r}{h}\right)^4-\left(\frac{1}{16}\right)\left(\frac{r}{h}\right)^5}$$

Where r= radius of the sphere, h= distance of the sphere centre from the wall.

Since we recorded the velocity of the beads at the surface, a valid estimate of h can be h=r, an assumption that the sphere is rolling on the surface. The force at 1.6A after correction would therefore be 22.48pN, which is more than thrice the obtained force. However, this has to be experimentally validated. The fact that this also differs from the 9.2pN value of simulated force (at 1.6A) is a concern and will be investigated.

An immediate priority is therefore to calibrate the instrument with beads in a solution whose density is equivalent or higher than that of the beads (i.e.1.6gm/cc). This would ensure that the beads remain neutrally buoyant giving a proper estimate of

force. Also, any non-uniformity in the z-axis can be more easily detected, since sinking of the beads due to gravity is now eliminated. We intend to use 3.9 M Cesium chloride solution (Fallesen et al., 2010) which has a density of 1.6gm/cc (Lyons and Riley 1954) and therefore would be suitable for this purpose.

Direction of magnetic force

The region focussed upon to track a bead within the capillary was +30µm to +150µm along the y-axis. This was primarily because beads beyond +30µm tended to deviate towards the magnet (to the left in Fig. 2.9) in the positive y-direction. The width of the capillary spans 300µm i.e. 150µm on either side of the y-axis. Ideally according to the pole piece design, beads present over a span of 250µm on either side of the centre should experience a uniform gradient along the x-axis. However, the x-y trajectory of the beads was parallel to x only in the area focussed.

This can be attributed due to an inherent asymmetry in the pole pieces. The araldite used for sticking the pole piece sheets in both magnets had a finite thickness that contributed differentially to the final thickness of individual pole pieces of the 2 magnets. An improvement over this would be to use a liquid variant of the araldite (that can tolerate temperatures upto 80^0C and is fine for our purpose since we do not intend to drive more than 1.6A current through the magnets.). In our case the pole piece to the left was thinner, concentrating more flux lines in a smaller area which would ultimately contribute to a greater field than the one to the right. This might have caused the observed deviation. Another cause might also be slight deviations in placement of the capillary at the exact centre of the pole pieces during experiments, due to errors in perceiving the distinct edges of the pole piece under the 10X objective.

Aggregation of beads.

All these experiments were done using a relatively dilute solution of beads (1.2×10^6 beads/ml or lower). A pertinent problem in concentrated solutions is that magnetic beads aggregate together when in close proximity (within 10-20µm of each other), when the field is on, due to dipole-dipole attractions. This dipole-dipole interaction, often accelerates or deviates a single bead's trajectory towards already existing aggregates of beads. This is especially evident from the trajectories of beads which

begin motion nearer to one wall of the capillary and eventually reach the walls and move along it or attach to other beads moving along the walls. Their presence affects the trajectory of beads near the centre which ideally in the absence of these beads at the wall would have moved straight. Such events might sometimes account for the slight deviations in x-y trajectories observed in tracked beads, even though the magnetic force in the region is parallel to x. Single beads as well as aggregates eventually gather and come to a stop at x=0, and reside at either wall of the capillary, even in dilute solutions. The presence of such a 'magnet' accounts greatly for the subsequent early deviation of single beads to either capillary wall. The region x=-5mm ± 1.5mm is a suitable region since it not only provides an appropriate gradient value but beads in this region are also fairly away from the influence of stationary bead aggregates at x=0.

Future work

The above-mentioned issues can be corrected for. Future work would involve:-

1. Using a 3.9M Cesium Chloride solution of beads to calibrate the trap by recording the velocity of neutrally buoyant beads.

   This would also aid our understanding of the force profile along the z-axis in the absence of gravity and help pinpoint whether friction with the surface may have caused the variation of velocity within a bead upto 4μm/s in some cases.

2. Accounting for the discrepancy between simulated forces and the faxen corrected values of force.
3. Preparing magnetic phagsomes with Dynal beads from dictyostelium cells and obtaining magnetic phagosome motility in-vitro.
4. Successful calibration of the instrument will be followed by probing the profile of single and multiple dynein-driven magnetic phagosome motion under constant load.

REFERENCES

Andreas R. Bausch, Winfried Moller and Erich Sackmann (1999). Measurement of Local Viscoelasticity and Forces in Living Cells by Magnetic Tweezers. Biophysical Journal , *76* 573–579

A Rais and A A Yousif (1999) A comparative study on the calibration of pole caps for a Faraday vacuum microbalance. Meas. Sci. Technol. *10*, 744–747

B. G. Hosu, K. Jakab, P. Banki, F. I. Toth, and G. Forgacs (2003) Magnetic tweezers for intracellular applications Rev. Sci. Instrum. *74*, 4158

C. Bean and J. Livingston (1959) γ-Fe_2O_3 nanoparticles dispersed in porous Vycor glass: A magnetically diluted integrated system. J. Appl. Phys. *30***, S120**

Chungil Ha, H. Daniel Ou-Yang and Hyuk Kyu Pak(2009). Study of a colloidal sphere near flat walls using oscillating optical tweezers Proc. of SPIE *7507*, 750502-1

Claudia Veigel and Christoph F. Schmidt (2011). Moving into the cell: single-molecule studies of molecular motors in complex environments. *12,* 163-176.

D. E. Soule C. W. Nezbeda A. W. Czanderna (1964) High Sensitivity Faraday Susceptibility Apparatus Rev. Sci. Instrum. 53, 1504.

F. H. C. Crick and A. F. W. Hughes (1950) The Physical Properties of Cytoplasm: A Study by Means of the Magnetic Particle Method, Part I. Experimental." Experimental Cell Research 1: 37-80

Gee, M.; Vallee, R., (1998) The role of the dynein stalk in cytoplasmic and flagellar motility. European Biophysics Journal with Biophysics Letters, 27, (5), 466–473.

G. Fonnum, C. Johansson, A. Molteberg, S. Morup, and E. Aksnes (2005) Characterisation of Dynabeadss bymagnetization measurements and Mossbauer spectroscopy Journal of Magnetism and Magnetic Materials. *293*, 1, 41-47

Gosse, C.; Croquette, V. (2002) Magnetic tweezers: Micromanipulation and force measurement at the molecular level. Biophysical Journal, 82, (6), 3314–3329.

Happel, J. and Brenner H. (1991), Low Reynolds Number Hydrodynamics, Kluwer, Dordrecht

I. D. Vilfan, J. Lipfert, D. A. Koster, S. G. Lemay, and N. H. Dekker (2009). Magnetic Tweezers for Single-Molecule Experiments. Handbook of Single Molecule Biophysics, Chapter 13.

K.C. Neuman, T, Lionnet, and J.-F. Allemand (2007) Single-Molecule Micromanipulation Techniques. Annu. Rev. Mater. Res. *37*:33–67.

Keir C Neuman and Attila Nagy, Nature (2005) Single-molecule force spectroscopy: optical tweezers, magnetic tweezers and atomic force microscopy. *5*, No. 6 491-505

Mallik, R.; Carter, B. C.; Lex, S. A.; King, S. J.; Gross, S. P.(2004), Cytoplasmic dynein functions as a gear in response to load. Nature, *427*, (6975), 649–652.

Manoranjan P. Singh, Roop Mallik, Steven P. Gross, and Clare C. Yu(2005) Monte - Carlo modelling of single-molecule cytoplasmic dynein. Proceedings of National Academy of Sciences, *102*, 34- 12059-12064

M. Garber, G. Henry, and H. G. Hoeve (1960) A Magnetic Susceptibility balance and the temperature dependence of the magnetic susceptibility of copper, silver and gold, 295^0-975^0 K. Canadian Journal of Physics . *38*, 1595-1613.

R.Conroy ()Force Spectroscopy with Optical and Magnetic Tweezers

Terence Strick, Jean-Francois Allemand, Vincent Croquette, David Bensimon (2000), Twisting and stretching single DNA molecules Progress in Biophysics & Molecular Biology 74, 115-140

T. L. Fallesen, D. B. Hill, M. Steen, J. C. Macosko, K. D. Bonin, and G. M. Holzwarth, (2010) Magnet pole piece design for uniform magnetic force on superparamagnetic beads. Rev. Sci. Instrum. *81*, 074303.